

# Integrated Framework for Artificial Immunity-Based Aircraft Failure Detection, Identification, and Evaluation

Mario G. Perhinschi,\* Hever Moncayo,† and Jennifer Davis‡  
*West Virginia University, Morgantown, West Virginia 26506*

DOI: 10.2514/1.45718

**This paper presents a novel conceptual framework for an integrated set of methodologies for the detection, identification, and evaluation of a wide variety of failures of aircraft subsystems based on the artificial immune system paradigm. The detection represents the capability to declare that a failure within any of the aircraft subsystems has occurred. The identification process determines which element has failed. The evaluation of the failure addresses three aspects: the type of the failure, its magnitude, and the reassessment of the generalized flight envelope. Failure detection, identification, and evaluation schemes are included using the bioimmune system metaphor combined with other artificial intelligence techniques. The immunity-based fault detection operates in a similar manner as does the immune system when it distinguishes between entities that belong to the organism and entities that do not. The proposed approach directly addresses the complexity and multidimensionality of aircraft dynamic response in the context of abnormal conditions and provides the adequate tools to solve the failure detection problem in an integrated and comprehensive manner. A multiself failure detection and identification scheme is presented for actuator, sensor, engine, and structural failures/damages, which was developed and tested using a motion-based flight simulator. The scheme achieves excellent detection rates and a low number of false alarms and demonstrates the effectiveness of the proposed framework.**

## I. Introduction

**F**AILURES and damages of aircraft subsystems have been identified throughout the years as a leading source of accidents for both military and civilian aircraft [1–4]. Timely detection and availability of automatic compensation capable of handling upset/abnormal situations can drastically increase the safety of aircraft operation [5]. Fault-tolerant flight control systems [6,7] have in recent years been the focus of significant research efforts for the development of technologies that may allow an aircraft to avoid unrecoverable postfailure flight conditions, regain equilibrium, and continue the mission. Many of these systems are based on the availability of failure detection, identification, and evaluation (FDIE) schemes to trigger compensating changes in the control laws. Information about occurring failures provided by FDIE schemes to the pilot can significantly improve his/her reaction time and, in turn, enhance the success probability for the postfailure recovery.

Physical redundancy for the actuators of the primary control surfaces is rarely available due to cost and added complexity and weight. Therefore, actuator failures for primary control surfaces may represent major threats to flight safety. Conversely, due to the lower cost and weight of the sensors, flight control systems typically rely on multiple physical redundancies in the sensors. However, for specific types of aircraft for which reduced complexity, reduced weight, and/or reduced costs are critical design issues, it may be appealing to design a flight control system without physical redundancy in the sensor components with some form of analytical redundancy from real time online estimates of the dynamic variables. Regulations require that multiple engine aircraft be capable of safe operation if one engine fails. However, information regarding the occurrence of the failure, location, and evaluation of the effect on reducing the envelope are necessary for the pilot and the control system. Structural

failures/damages can vary from minor to catastrophic and can potentially have a significant effect on the aerodynamics and hence the control and performance of the aircraft.

The number of potential abnormal situations, each exhibiting very different dynamic signatures, is very large. Their specific characteristics and circumstances are potentially so numerous and their individual chances of occurrence are so low that it is not feasible to train pilots in an exhaustive manner, due to time and cost constraints, to handle all the nonnominal situations associated with each class of failures/damages/malfunctions. The existence of an FDIE scheme can support automatic accommodation as part of a fault-tolerant control system and it can also improve human accommodation through increased pilot situational awareness.

Most of the research efforts in the area have focused on individual classes of failure and did not address the failure evaluation aspect. State estimation or observer-based schemes have been widely proposed [8–11] for actuator failure detection and identification (FDI) relying on Kalman or other classes of filters. Artificial neural networks (ANN) have also been extensively used [12–15] to solve the FDI problem for aerospace systems. Alternative approaches for FDI and pilot awareness enhancement were also proposed based on inductive learning [16].

The issue of sensor FDI has been addressed to a lower extent, since triple and quadruple physical redundancy of aircraft sensors is a common practice. However, sensor FDI schemes based on ANN estimations of sensor outputs have been proposed [17,18].

Research regarding the dynamic impact and accommodation of structural damage to main aircraft components (wing, horizontal tail) has recently been focused on the development of fault-tolerant control laws [19] with indirect failure assessment through parameter identification without explicit FDIE. The use of large networks of sensors for global structural health monitoring is also investigated [20].

The failure evaluation process involves three aspects: determine the type and the magnitude/severity of the failure, and evaluate its effect on reducing the flight envelope, in the most general sense. These issues are important to enhance pilot situational awareness and provide necessary information to the automatic control system to avoid commands that might lead to loss of control and other dangerous/catastrophic situations.

The attempt to integrate FDIE for a large diversity of aircraft subsystems and over extended areas of the flight envelope poses

Received 29 May 2009; revision received 1 April 2010; accepted for publication 24 August 2010. Copyright © 2010 by M. G. Perhinschi. Published by the American Institute of Aeronautics and Astronautics, Inc., with permission. Copies of this paper may be made for personal or internal use, on condition that the copier pay the \$10.00 per-copy fee to the Copyright Clearance Center, Inc., 222 Rosewood Drive, Danvers, MA 01923; include the code 0021-8669/10 and \$10.00 in correspondence with the CCC.

\*Assistant Professor, Department of Mechanical and Aerospace Engineering. Senior Member AIAA.

†Graduate Student, Department of Mechanical and Aerospace Engineering.

significant challenges. From a failure accommodation point of view, the differentiation between, for example, a sensor and an actuator failure is a critical task because different types of compensation are necessary in each case. If the specific signal associated with the sensor failure is used in the control laws, it might be challenging for a pilot to distinguish between sensor and actuator failures. Furthermore, very often, it is important but difficult to determine, within each of the two categories, which particular element has failed. Such issues related to the integration of FDIE for different classes of failure have only been addressed on a limited basis [18,21] and comprehensive and systematic methodologies have yet to be developed.

The need for a solution to the FDIE problem for aerospace vehicles that includes all subsystems over the entire flight envelope has been widely acknowledged [22–25] and has become a major objective of NASA's Aviation Safety Program [5]. The complexity and extremely high-dimensionality of the problem require adequate tools. Recently, a new concept inspired from the biological immune system was proposed for aerospace systems FDI [26,27]. The artificial immune system (AIS)-based fault detection operates in a similar manner as does its biological counterpart, according to the principle of self/nonself discrimination, when it distinguishes between entities that belong to the organism and entities that do not. This paradigm can potentially directly address the complexity and multidimensionality of aircraft dynamic response in the context of abnormal conditions and provide the tools necessary for a comprehensive/integrated solution to the FDIE problem. In this paper, the development at West Virginia University (WVU) of a novel integrated framework for the detection, identification, and evaluation of a wide variety of sensor, actuator, propulsion, and structural failures/damages is presented. This contribution is expected to provide a new perspective on the needed comprehensive/integrated solution to the FDIE problem beyond the limitations of current approaches. The bioimmune system metaphor is used, combined with other artificial intelligence techniques such as genetic algorithms, ANN, and fuzzy logic-based adaptive thresholds.

A brief review of the AIS paradigm and its application is presented in Sec. II. The general aspects of the FDIE problem for aerospace vehicles are formulated in Sec. III followed in Sec. IV by the description of the structure and architecture of the proposed solution framework. Sec. V provides details on the main processes such as the definition of the self/nonself, detector generation, FDIE logic, and others. An example of a multiself FDI scheme and a brief analysis of its performance are presented in Sec. VI. Finally, some conclusions are summarized in Sec. VII, followed by acknowledgments and a reference list.

## II. Artificial Immune System Paradigm

The biological immune system has the capability to detect exogenous entities while not reacting to the self cells. T-cells [28] are the component of the system with the most important role in this process. T-cells are first generated through a pseudorandom genetic

rearrangement mechanism, which ensures high variability of the new cells in terms of biological identifiers. Typically, these identifiers are specific molecular strings of organic compounds such as proteins or polysaccharides. A selection process takes place in the thymus resulting in the destruction of the T-cells whose identifiers match the self. Eventually, only those T-cells that are “different” are allowed to leave the thymus and proliferate. This process is referred to as *negative selection*. The surviving T-cells can now circulate throughout the body to detect intruders and mark them for destruction.

The mechanisms and processes of the biological immune system are the inspiration for the AIS, as a new artificial intelligence technique for fault detection [29–31]. The basic idea of this new computational paradigm is that an abnormal situation (i.e. failure of one of the aircraft subsystems, which is considered similar to an invasion by external bioagents) can be declared when a current configuration of identifiers or features does not match with any configuration from a predetermined set known to correspond to normal situations. These identifiers or features, similar to the chemical compounds that form the biological identifiers, represent the encoding of the self. They can include various sensor outputs, states estimates, statistical parameters, or any other information expected to be relevant to the behavior of the system and able to capture the signature of abnormal situations. Extensive experimental data are necessary to determine the self or the hyperspace of normal conditions. Adequate numerical representations of the self/nonself must be used and the data processed such that they are manageable given the computational and storage limitations of the available hardware. The artificial counterpart of the T-cells, the detectors, must then be generated and optimized. This process typically attempts to mimic the variation followed by selection of the T-cells. The process may be repeated to generate several sets of detectors as part of a hierarchical scheme that allows failure isolation and evaluation. Finally, a detection logic must be designed for real time operation with a high detection rate and low number of false alarms. The block diagram of the AIS design process for fault detection is presented in Fig. 1.

The AIS concept has shown a promising potential for a variety of applications [32] such as anomaly detection in computer operation [33,34], pattern recognition [35,36], data mining [37,38], computer security [30,39–41], and adaptive control [42,43]. KrishnaKumar and Dasgupta have pioneered the use of AIS for fault detection of aerospace systems [26,27].

Although new models and methods are currently being developed and existing ones are improved continuously, theoretical issues have only been addressed occasionally in the attempt to assess and prove AIS applicability [36,44,45] and the theoretical background to support the AIS is limited.

## III. Aircraft Subsystem FDIE Problem

It is desirable to perform the aircraft subsystem FDIE with the necessary level of detail to allow for adequate specific reformulation of the control tactics and strategies such that the control of the vehicle is maintained or recovered and the mission is continued with the

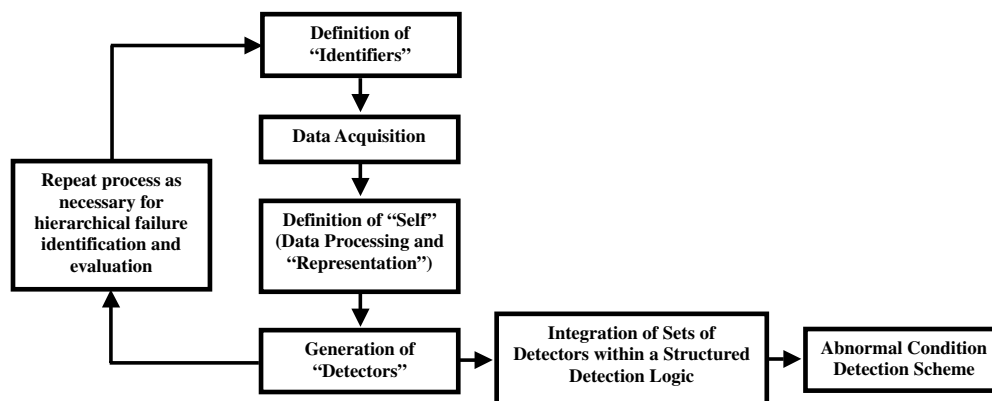


Fig. 1 AIS-based abnormal condition detection.

same or amended objectives and requirements. The three processes grouped under the acronym FDIE must be performed in subsequent phases to increase efficiency and reliability. Detection represents the process of declaring that a generic malfunction of the system has occurred. Any one or several of the total  $N_S$  subsystems can be subject to the failure. These subsystems can be actuators, sensors, propulsion, structural elements, etc. It should be noted that the concept of subsystem can be extended beyond the usual hardware to include software, the human pilot, and the environment. This would allow for the consideration of abnormal situations such as pilot fatigue, turbulence, or nonstandard atmospheric conditions. The identification process has two phases or more, depending on the complexity of the subsystems. The first phase consists of determining in which of the  $N_S$  categories the failure falls or, in other words, determining what is the failed subsystem. The outcome of the second phase specifies the failed element (e.g. roll rate sensor, or rudder actuator, or left wing). In certain situations, an intermediate phase could be defined to distinguish between groups within the subsystem. For example, if an actuator failure is declared, an intermediate phase would determine which of the three control channels is affected; let us say the longitudinal channel. Furthermore, the identification should specify if it is an elevator or a canard failure and eventually, if the right or left surface is affected. The evaluation of the failure addresses three aspects. One is of a qualitative nature and involves determining the type of the failure. For example, the qualitative evaluation is expected to determine if an actuator failure consists of a locked actuator, or a freely moving control surface, or a reduction of control efficiency. The other two aspects are of a quantitative nature and can be defined as direct and indirect. The direct failure evaluation consists of estimating the magnitude or severity of the failure (e.g., left aileron locked at  $+10^\circ$ ). The indirect failure evaluation includes the reassessment of the flight envelope and prediction of the limitations and constraints on the performance and handling qualities inflicted by the presence of the failure. The general aspects of the aircraft subsystem FDIE problem are illustrated in Fig. 2.

It is envisioned that the role of such a FDIE system will be twofold:

- 1) It will trigger compensatory actions from the fault-tolerant flight control system to maintain stability and control of the aircraft.
- 2) It will provide information to the pilot and/or control system for situational awareness and decision making regarding modification of control and navigation strategies.

#### IV. General Architecture of AIS-Based FDIE

Using the flowchart in Fig. 1 as a starting point, the aircraft subsystem FDIE based on the AIS paradigm can be considered to include three main processes: 1) preprocessing of information and flight data; 2) online detection, identification, and evaluation, and 3) postprocessing of FDIE outcomes.

The general flowchart of the AIS-based FDIE is presented in Fig. 3.

The preprocessing of information and flight data has as outcomes the sets of detectors for the various phases of the FDIE. This process includes key activities such as the definition of the identifiers, data acquisition, data reduction, and detector generation and optimization.

The online FDIE process implies the development and operation of the FDIE scheme. Sets of current values of the identifiers measured in flight at a certain sampling rate are compared against the detectors. For each sample, a binary output results, 0 if the current values of the identifiers are outside the detector (normal situation) or 1 if the current values are inside the detector (abnormal situation). Alternatively, an output between 0 and 1 can result if fuzzy instead of crisp boundaries are considered for the detectors. To reduce the number of false alarms, sets of output values over moving time windows are typically used to produce the FDIE outcome and declare a failure.

The postprocessing of FDIE outcomes and the analysis of false alarms and failed detections can potentially be used on or offline to alter the detector sets and improve the overall performance.

#### V. Description of Main AIS-Based FDIE Components

##### A. Definition of Identifiers

The success of the FDIE scheme will depend on the capability of the parameters selected as identifiers to capture the dynamic signature of each and every type of failure. The identifiers must be measured from flight tests, computed through simulation, or estimated. The candidate parameters for self/nonself definition can be selected from any, some, or all of the following five categories: 1) aircraft state variables, 2) pilot input variables, 3) stability and control derivatives, 4) variables generated within the control laws, and 5) derived variables.

The aircraft state variables are a natural choice since it is expected that they capture the fingerprint of many failure classes. In fact,

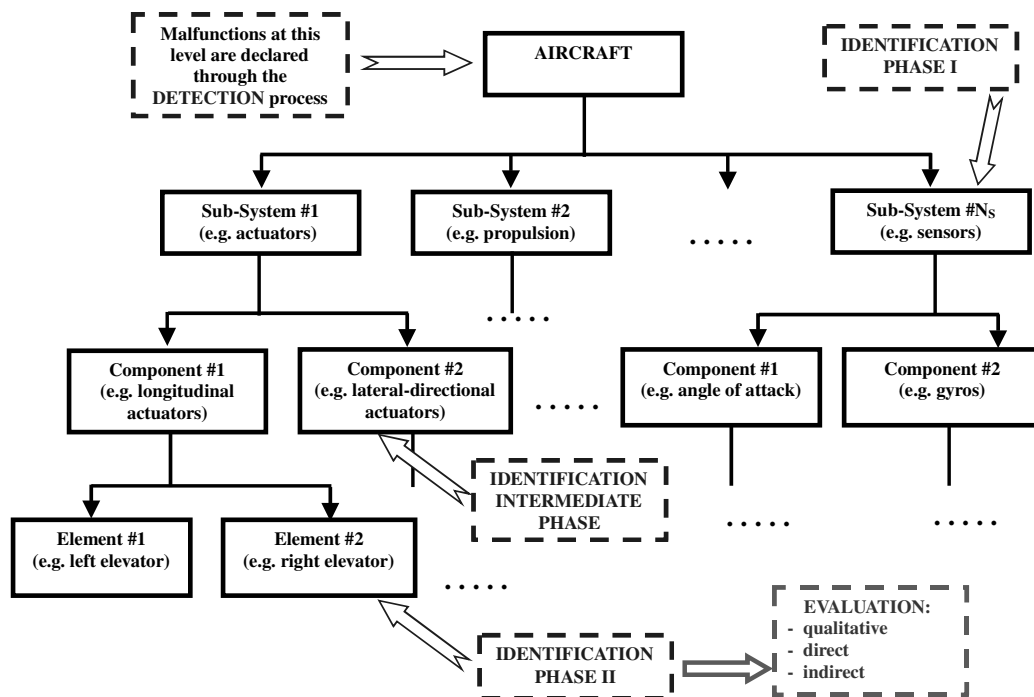


Fig. 2 Aircraft subsystem FDIE problem.

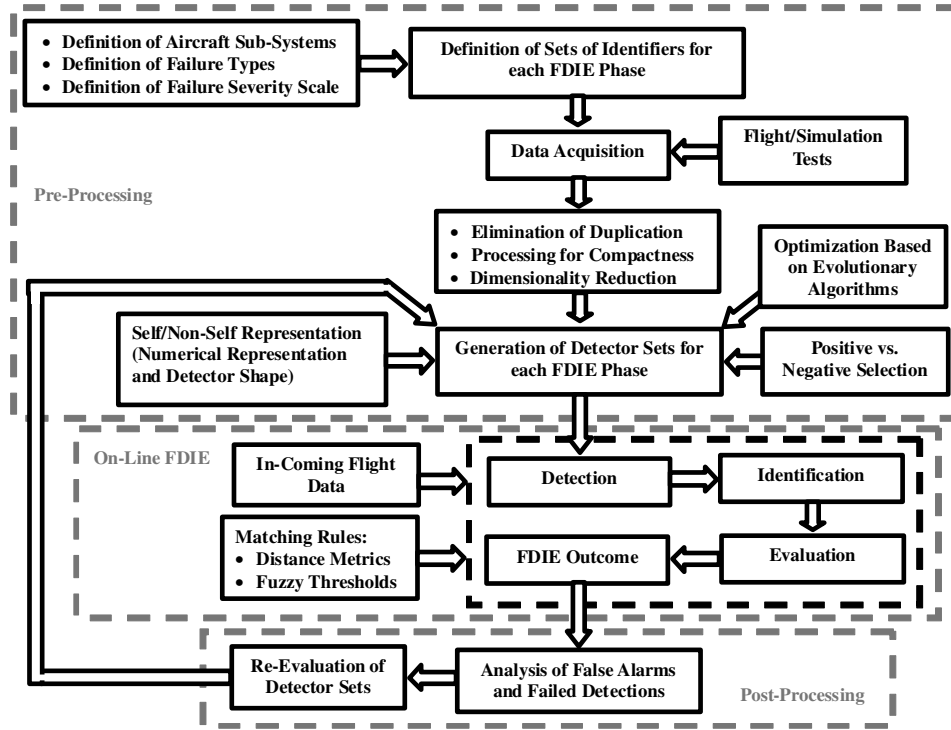


Fig. 3 AIS-based aircraft subsystem FDIE.

measurements of aircraft angular rates have been used for self/nonself definition and failure detection with promising results [27]. One potential limitation of using state variables alone as identifiers is the fact that it is possible to reproduce the dynamic fingerprint of a failure through intentional pilot input. For example, it is well known that an elevator failure induces a coupling between the longitudinal and lateral channel as a consequence of altered aircraft symmetry. This characteristic may be used for detection by using as identifiers roll and pitch rates. However, it is possible to achieve similar coupling under normal conditions through simultaneous pilot input on both channels. The locus of nondimensionalized roll and pitch rates is presented in Fig. 4 for decoupled lateral and longitudinal inputs at nominal conditions. Note that the crosslike shape is due to the decoupling: input on one channel produces an angular rate response on that channel only. The elevator failure will be responsible for nonzero roll rate in response to a longitudinal input, as shown in Fig. 5. However, a similar pattern of the locus can be obtained if simultaneous inputs are provided on both the lateral and longitudinal channel, as shown in Fig. 6. This example suggests that information about the pilot input may be needed for correct failure detection. Several signals can be used to provide such information: stick and pedals displacement, aerodynamic control surfaces deflections, and reference state variables generated by model following control laws.

The stability and control derivatives can provide useful information regarding subsystem failures. However, it should be noted that determining them online is not a trivial problem.

The use of adaptive control laws can provide additional signals with FDI capabilities. It is expected that the adaptation activity increases after the occurrence of a failure. Depending on the architecture of the adaptive control laws, signals that can capture this increased adaptation activity and thus detect the failure may include: adaptation rate, control compensation, neural network (NN) output and its derivative, and NN weights and their derivatives.

Previous studies [15,21,46] have put into evidence promising parameters for FDI based on correlations between state variables (angular rates) and neural estimates of the angular rates. For example, the main quadratic estimation error (MQEE) parameter is defined as

$$\text{MQEE}(k) = \frac{1}{2}[(p(k) - \hat{p}_{\text{MNN}}(k))^2 + (q(k) - \hat{q}_{\text{MNN}}(k))^2 + (r(k) - \hat{r}_{\text{MNN}}(k))^2] \quad (1)$$

where  $\hat{p}_{\text{MNN}}(k)$ ,  $\hat{q}_{\text{MNN}}(k)$ , and  $\hat{r}_{\text{MNN}}(k)$  are NN estimates of angular rates at time  $k$ , using measurements from time instant  $k-1$  to  $k-m$ . The inputs to the neural estimator include outputs of the respective gyros. Additionally, a NN output quadratic estimation error (OQEE) parameter is defined as

$$\text{OQEE}(k) = \frac{1}{2}[(\hat{p}_{\text{DNN}}(k) - \hat{p}_{\text{MNN}}(k))^2 + (\hat{q}_{\text{DNN}}(k) - \hat{q}_{\text{MNN}}(k))^2 + (\hat{r}_{\text{DNN}}(k) - \hat{r}_{\text{MNN}}(k))^2] \quad (2)$$

where  $\hat{p}_{\text{DNN}}(k)$ ,  $\hat{q}_{\text{DNN}}(k)$ , and  $\hat{r}_{\text{DNN}}(k)$  are neural estimates which do not use outputs of the respective gyros. Another example is the angular rate correlation parameter defined as [21]

$$\bar{R}_{pqr}(k) = \sum_{i=k-n_R}^k R_{pq}(i) + \bar{\mu}_{rr} R_{rr}(i) \quad (3)$$

where  $R_{pq}$  is the cross-correlation between roll and pitch rate,  $R_{rr}$  is the autocorrelation of the yaw rate, and  $\bar{\mu}_{rr}$  is a scaling factor.

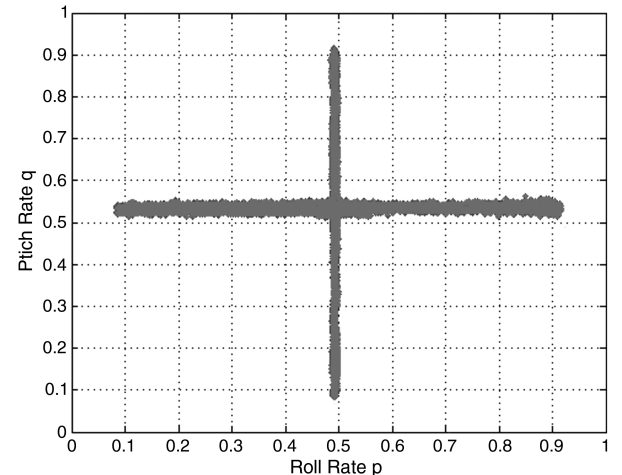


Fig. 4 Longitudinal and lateral decoupled input: nominal condition.

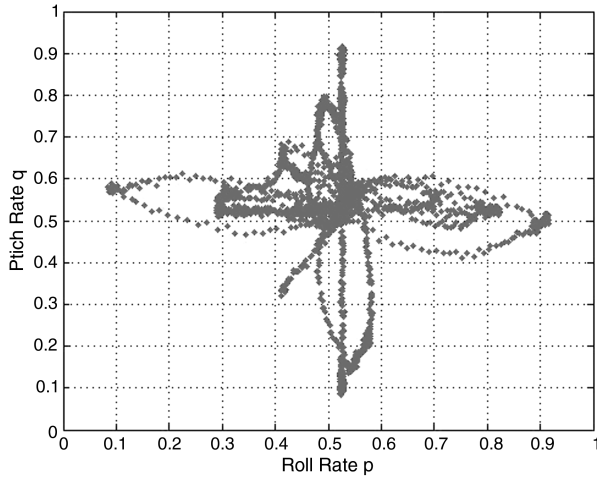


Fig. 5 Longitudinal and lateral decoupled input: elevator failure.

The impact of selecting different identifiers on the performance of the detection is illustrated [47] in Figs. 7 and 8. All the examples in this paper were obtained using a customized simulation environment [48] build around the WVU six degrees-of-freedom motion-based flight simulator. The mathematical model of a supersonic fighter is used including models of a variety of subsystem failures and fault-tolerant control laws based on nonlinear dynamic inversion and artificial NN augmentation [18]. For all cases presented in this section, the false alarms and detection rates have been calculated as the percentage of all nominal data points and all data points at abnormal conditions, respectively, that fall inside the nonself regions of the hyperspace. The sampling rate for all tests is 50 Hz. To determine the false alarms, nominal data were used that are different than those used in the detector generation process. The following identifiers were considered for the definition of the self: 1) self 1: NN roll channel weight, NN compensation on all three channels, and derived parameters (MQEE, OQEE, and others),  $Rpq$ ,  $Rrr$ , and tracking errors on all three channels (14-dimensional space); 2) self 2: NN roll channel weight, NN compensation on all three channels, and derived parameters (MQEE, OQEE, and others) (nine-dimensional space); 3) self 3: NN roll channel weight, NN compensation on all three channels (four-dimensional space); and 4) self 4: tracking errors on all three channels (three-dimensional space).

Differentiating between numerous classes of failures requires a large number of identifiers thus increasing the dimensionality of the detector space and exposing the entire process to specific issues [49,50] that can potentially have a negative impact on the performance of the FDIE scheme. When increasing the dimensionality of the self/nonself space, an exponentially larger number of clusters/

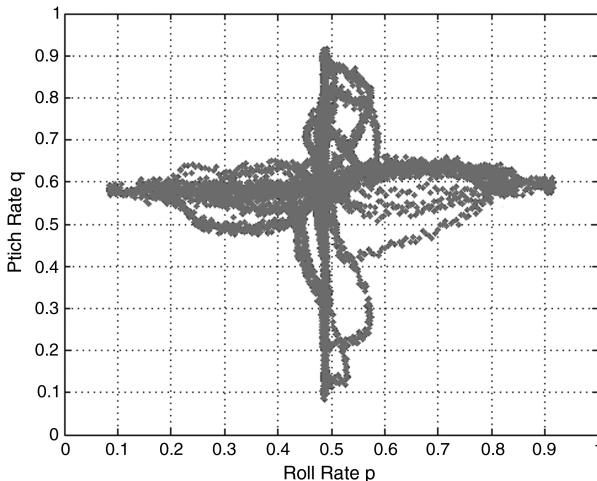


Fig. 6 Longitudinal and lateral coupled input: nominal condition.

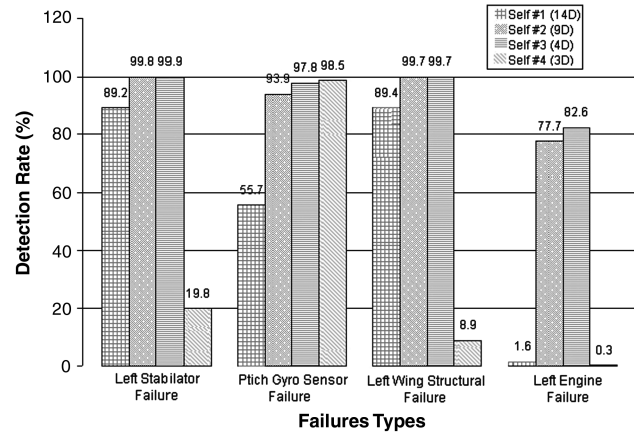


Fig. 7 Detection rates of different sets of identifiers.

detectors are necessary to maintain the same resolution. This requirement was not met in the tests presented in Figs. 7 and 8 as the same number of clusters was used for all cases, which resulted in larger clusters for the 14-dimensional set and in more empty space/nonself included in them leading to the lower performance of the highest dimensionality identifier set. Dimensionality reduction techniques [51] may be used to avoid effects of high dimension spaces while preserving the quality of information. In general, a larger number of detectors is expected to achieve a better coverage of the nonself, hence better detection performance (as shown in Fig. 9) at the expense of computational effort. However, it should be noted that a larger number of detectors is typically accompanied by a reduction in the size of (some) detectors. The implication is that smaller size detectors are more likely to cover small areas in the vicinity and between the self clusters, areas that very often are actually self for which data is not available. As a consequence, the false alarm rate may increase along with the number of detectors, as supported by the results shown in Fig. 10.

## B. Data Acquisition and Processing

Selecting the right set of identifiers is only a necessary condition for a complete and accurate description of the self. Adequate coverage of the state space must also be achieved. Different flight scenarios including representative maneuvers must be performed over, ideally, the entire flight envelope and data recorded and stored. Large amounts of experimental data are necessary to determine the self or the hyperspace of normal conditions. The issues of the quantity and quality of the data to be used for self definition must be considered carefully. The number of tests necessary may be reduced if it is determined that the region of the hyperspace for a given set of identifiers and range of additional flight parameters does not expand when the additional parameters take values outside the initial range. If simulation data are used, the simulation model must be accurate enough not to produce self/nonself overlapping. The self/nonself

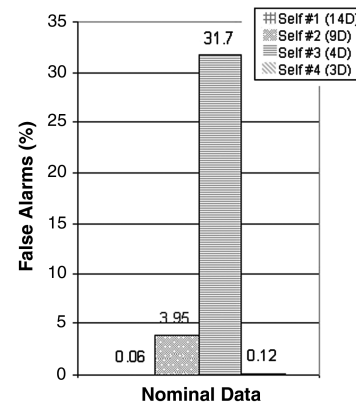


Fig. 8 False alarms of different sets of identifiers.

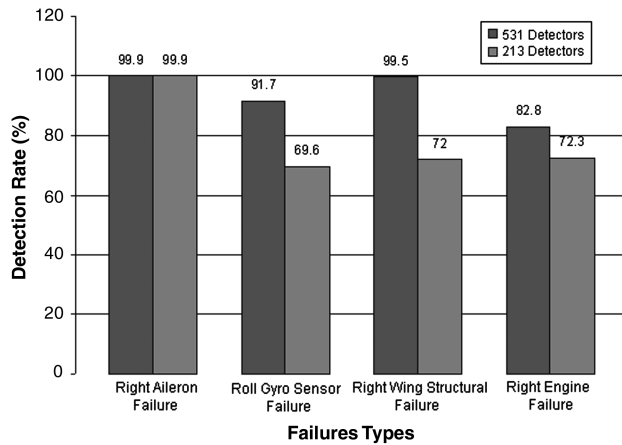


Fig. 9 Detection rate using different number of detectors.

consists of sets of  $n$ -dimensional points representing all combinations of selected  $n$  variables (identifiers). For aircraft subsystem FDIE, these sets of points are the collection of all time histories over the entire flight envelope. Since the distance between the points is critical for the detection process, different scales of the identifiers is not desirable; therefore, the data must be normalized. To reduce the size of such a large database, two methods are used: 1) clustering of data and condensed representation and 2) elimination of data duplication.

Condensed representation using a reduced number of parameters can be achieved by replacing clusters of data by circumscribed geometrical hyperbodies. This representation of a cluster will include a (potentially) large number of data points (self) but also a certain amount of “empty space”, points between the actual data, which are assumed to be “self” but can actually be either self or “nonself.” When evaluating the amount of empty space, a certain confidence radius is assumed around every self point within which all points are considered self. This is another parameter that must be selected with caution. Pertinent values for this radius can be obtained by analyzing the distance between points of the self measured at different sampling rates. If a small number of clusters are generated, in order to cover all data points, the size of every cluster will likely be large compared with the radius around each data point and a large amount of empty space, potentially nonself, is included. In Fig. 11, the variation of the empty space with the number of clusters is presented. In this example, a number of 26831 self data points (pairs of pitch and roll rate values from flight simulation) and a constant self point confidence radius of 0.0005, normalized with respect to the unit hypercube, are considered. The empty space decreases when the number of clusters is increased. Note that the empty space can reach significantly large values.

The characteristics (shape) of these hyperbodies have an impact on the efficiency of the detector generation process and on the detection itself. They determine how well the nonself is covered, how

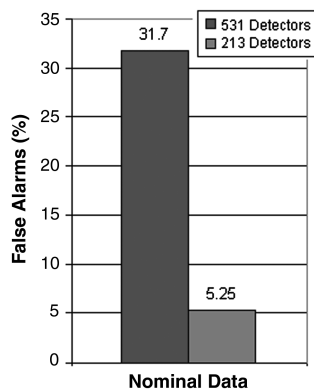


Fig. 10 False alarms using different number of detectors.

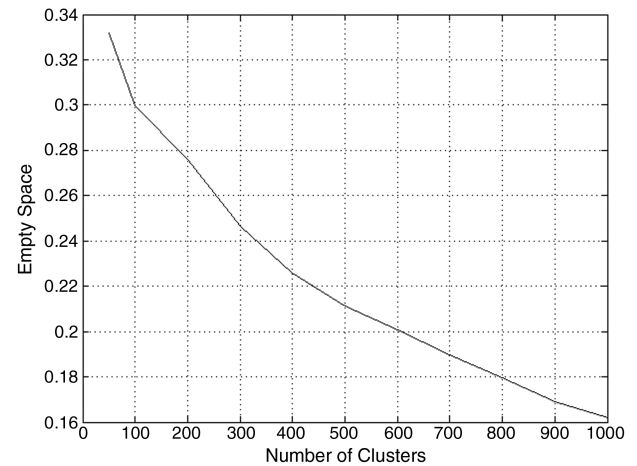


Fig. 11 Variation of empty space with total number of clusters.

many detectors are necessary, and how intensive the computational process is.

The following shapes for the self/nonself can typically be considered: 1) hypercubes, determined by an  $n$ -dimensional center and one value for the size; 2) hyperrectangles, determined by an  $n$ -dimensional center and  $n$  values for the size; 3) hyperspheres, determined by an  $n$ -dimensional center and one value for the radius; 4) hyperellipsoid of rotation, determined by an  $n$ -dimensional center and two values for the axes [52]; and 5) generalized hyperellipsoid, determined by an  $n$ -dimensional center and  $n$  values for the axes.

For all shapes (except hyperspheres) variable orientation can be considered as determined by an additional  $n$ -dimensional vector.

To illustrate the potential impact on performance of selecting the hypershape, self 4 was used to generate detectors using hyperspheres and hyperrectangles of variable sizes. 500 detectors were generated and the detection results considering different types of failures are shown in Fig. 12. In general, the detection rate remains around the same for the two hypershape cases. However, a lower number of false alarms are achieved using hyperrectangle antibodies. This is due to the fact that because of the allowed overlapping, the spherical detectors achieve better coverage of the nonself including areas that are attributed to the nonself simply because of imperfections of the self. Thus, for the same number of hyperrectangles, the hyperspheres produce an increase of the number of false alarms. In the literature, a combination of different hypershapes in an integrated scheme has been proposed [53]. As compared with existing single-shaped detection strategy, the approach utilizes the geometric properties of each shape to improve the detection performance in terms of coverage, number of detectors generated and overlap constraints by adding geometric flexibility and diversity.

Data representation has an important impact on algorithm effectiveness and performance. It determines the possible matching rules, the detector generation mechanisms, and the detection process. In general, the data to be processed may include numeric data, categorical data, Boolean data, and textual data. Data representation schemes can be grouped into two basic types: string representation and real-valued vector representation. In string representation, a detector is represented as a string over a finite alphabet. The length of the string is usually fixed, but it can also be variable. All four data types mentioned above can be processed using the string representation. Binary representation is a special case of string representation that is widely used for AIS applications [54]. Because of the binary implementation within computers, the binary representation may be considered to subsume all other representations. However, a matching rule defined on a high-level representation generally does not translate into a binary matching rule or rules in a straightforward way. It is important for the proper processing of the data that the matching rule reflects the actual Euclidean distance between the components tested [55]. Within the real-valued vector representation, each data item is a vector of real numbers [56,57]. The matching rules and the measure of difference or similarity are based on the

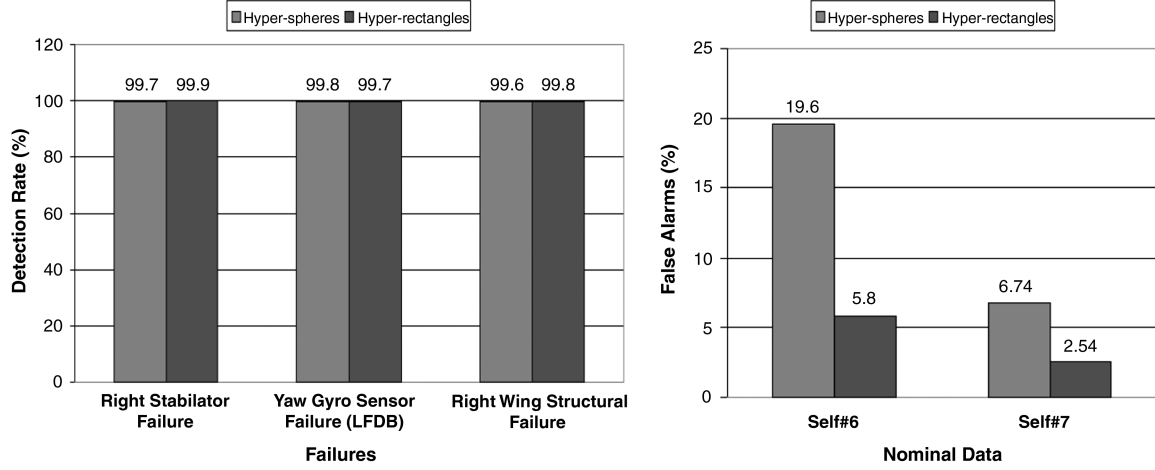


Fig. 12 Detection rate and false alarms for different hypershape detectors.

numeric elements of the vector. Hybrid representations combining strings and real-valued vectors exist also [58,59] where each data instance may consist of several features of different data types such as integer, real value, categorical information, Boolean value, text information, etc.

To define the self, numerous flight tests must be performed and flight data recorded over different conditions within the normal flight envelope. Duplication of flight conditions can easily occur. It is also possible that combinations of values of specific sets of identifiers be identical within a threshold for different flight conditions. This situation is more likely to occur for low dimension sets of identifiers. In any case, in order to reduce the storage space and computational effort, data redundancy must be eliminated.

### C. Detector Generation Optimization Metrics

The intersection between the self clusters and nonself detectors must ideally be the empty set. If there is enough test data to define the self, the clustering process may inadequately introduce into the self regions, the nonself and negatively impact the detection rate. If enough data is not available and/or the detector generation process allows for the detectors to overlap with the self, then the false alarms rate is likely to be high.

When the self clusters contain more than one data point, there will necessarily be some empty space, which is attributed to the self but could actually belong to the nonself. The presence of empty space is likely to reduce the detection rate and must be minimized.

Incomplete coverage of the nonself by the detectors will allow for some failures to be regarded as normal conditions and the detection rate is reduced.

Overlapping among self clusters and among nonself detectors does not impact the detection and false alarms rates; however, it can potentially reduce the efficiency of the scheme requiring more memory space and computational time. The number of clusters and detectors has a similar effect on the computational efficiency. Generally, the same space can be covered by many small detectors or fewer large detectors. For calculation purposes, it is better to have fewer detectors. For the detection of wider classes of abnormal conditions, large detectors may prove successful; however, for identification purposes, in particular, to distinguish between failures that are close to each other in the variable space, higher resolution may be necessary that can be achieved with smaller detectors.

To summarize, the following optimization criteria should be considered when generating the detectors [60]: 1) no overlapping among nonself detectors and self; 2) minimum empty space in the self clusters; 3) minimum uncovered areas in the nonself; 4) minimum overlapping among self clusters; 5) minimum overlapping among nonself detectors; and 6) minimum number of detectors (note that this criterion may be constrained by imposing a maximum size for the detectors in order to achieve a desirable resolution).

### D. Detector Generation via Negative Selection

Via the negative selection strategy [30] (NSS), detectors are generated such that they coincide with the nonself. The approach is inspired by the mechanism used by the biological immune system to train the T-cells to recognize antigens (nonself) and prevent them from recognizing the body's own cells (self). The AIS attempts in this way to differentiate between what is normal and what is abnormal.

In general, the real-valued NSS fills the nonself space with detectors and declares currently explored configurations to be abnormal if they lie within any detector. Structuring the nonself creates premises for the identification, as described in Sec. V.F.

There has been, to date, no research reporting on the deterministic generation mechanism for real-valued vector representation. Therefore, the current approaches rely on random initialization of candidate detectors and subsequent censoring to achieve one or more of the requirements outlined in the previous subsection.

An enhanced NSS detector generation algorithm has been developed using hypersphere real-valued representation and variable detector size and used for all examples in this paper. An initial set of candidate detectors is located randomly to cover the  $n$ -dimensional nonself hyperspace. Next, the algorithm performs an iterative selection process based on two criteria: no overlapping with the self and maximum coverage of the nonself. At each iteration, the radius of each detector is computed using the distance between the center of the candidate detector and the nearest self cluster. Since a minimum radius  $r_m$  is permitted for detectors, the distance between centers  $d(c_i, c_j)$  must be greater than or equal to the sum of  $r_m$  and the radius of the cluster  $r_c$ . Because of the geometric shape of the detectors, perfect coverage can only be reached if some overlapping between detectors occurs. An overlapping measure  $w_i$  of a detector with respect to the others is calculated during the maturation process [27]:

$$w_i = \sum_{j=1}^m (e^{\delta_{ij}} - 1)^{n-1} \quad (4)$$

where

$$\delta_{ij} = \left( \frac{r_i + r_j - d(c_i, c_j)}{2r_i} \right) \quad (5)$$

For an overlapping threshold value  $w_{thr}$ , every detector is selected as mature if the condition  $w_i \leq w_{thr}$  is satisfied. Eventually, if  $w_i = 0$ , that particular detector is selected to have a number of  $N_{clon} = 2n$  clones around it. The center of the first clone is placed at a distance equal to one radius and with a random orientation. The remaining clone centers are generated at  $90^\circ$  angles with respect to the first one. If  $0 < w_i \leq w_{thr}$ , only one center clone is generated along a direction opposite to nearest element (mature detector or self cluster), according to

$$c_{\text{clone}} = c_{\text{mature}} + (1 + \eta_{\text{clone}}) r_{\text{mature}} \frac{c_{\text{mature}} - c_{\text{nearest}}}{\|c_{\text{mature}} - c_{\text{nearest}}\|} \quad (6)$$

where  $\eta_{\text{clone}}$  corresponds to a decay parameter which determines how far the clone element is located at every iteration and is defined by

$$\eta_{\text{clone}} = \eta_{\text{clone}0} e^{-\text{iter}/\tau_{\text{clone}}} \quad (7)$$

Additionally, the  $N_{\text{MOV}}$  smallest rejected detectors are selected to be moved in the opposite direction of the mean center of the  $k$  nearest elements. The new centers are repositioned at

$$c_{\text{mov}} = c_{\text{rejec}} + \eta_{\text{clone}} \frac{c_{\text{rejec}} - c_{\text{nearest}}}{\|c_{\text{rejec}} - c_{\text{nearest}}\|} \quad (8)$$

Finally,  $N_{\text{RD}}$  random centers are inserted; the radius of the mature detectors calculated, and the coverage and overlapping computed by using a Monte Carlo method [61].

The process can be stopped after a prescribed number of iterations, when a prescribed maximum number of acceptable detectors has been reached, or when a desired coverage of the nonself has been achieved. The algorithm can optimize the requirements for no overlapping among nonself detectors and self and minimum uncovered areas in the nonself.

### E. Detector Generation via Positive Selection

Through the positive selection strategy (PSS), the detectors are generated to coincide with the self and the process is equivalent to clustering the self data and representing the clusters as hyperbodies of adequate shape. This time, an abnormal situation is declared if any of the currently explored configurations does not match any of the detectors. Through the PSS, the generation of nonself detectors and the high-dimensionality issues related to it are avoided [44,45]. However, the additional flexibility of NSS for identification purposes is lost.

### F. FDI Logic

#### 1. Matching Rules

A process that is of absolute importance for the AIS is the matching between the detectors and the explored data or candidates (data subject to the detection process). This is the equivalent of the biological matching between the antibodies and antigen, which is the basis for the recognition and selective elimination mechanism of foreign elements. In general, the matching rules rely on metrics for comparison and logic to produce a binary output: match or not-match. They depend on the type of data representation. The matching rules are used in two instances. First, there is the detector generation process (for NSS), in which candidate detectors are compared with the self. Second, there is the detection process, during which the explored data are compared with the established detector set to check for abnormalities.

One of the first matching rules based on binary representation implemented for AIS is the so-called  $r$ -contiguous matching [30]. The matching between detectors and candidates is declared positive if there is a window of preselected size  $r$  in which all the bits are identical. Alternative matching rules have been proposed using binary programming [34] and binary measures of distance or similarity [62].

The real valued vector representation describes the self/nonself as sets of  $n$ -dimensional points; therefore, in general,

$$\text{Candidate} = C = [c_1, c_2, \dots, c_n]^T, \quad C \in \mathbb{R}^n \quad (9)$$

$$\text{Detector} = D = [d_1, d_2, \dots, d_n]^T, \quad D \in \mathbb{R}^n \quad (10)$$

The matching rules are based on the “distance”  $\Delta$  between  $C$  and  $D$ .  $\Delta$  can be defined as the Minkowski distance:

$$\Delta(C, D) = |C - D|_p = \left( \sum |c_i - d_i|^p \right)^{\frac{1}{p}} \quad (11)$$

with its particular case, the Euclidean distance, for which  $p = 2$ .

The matching rule can be defined in terms of a distance threshold  $\delta_d$ :

$$\Delta \leq \delta_d \Rightarrow \text{match} \quad (12)$$

Alternatively, a detection radius  $\rho_d$  is defined and the matching rule formulated as

$$\Delta < 2\rho_d \Rightarrow \text{match} \quad (13)$$

This is equivalent to describing the self/nonself as a set of hyperspheres. In this case, a candidate or detector becomes

$$\text{Candidate} = C = \{O_C, R_C\}, \quad O_C \in \mathbb{R}^n, \quad R_C \in \mathbb{R} \quad (14)$$

$$\text{Detector} = D = \{O_D, R_D\}, \quad O_D \in \mathbb{R}^n, \quad R_D \in \mathbb{R} \quad (15)$$

where  $O$  are the centers and  $R$  the radii of the respective hyperspheres. The matching rule can be formulated as

$$\Delta(O_C, O_D) < R_C + R_D \Rightarrow \text{match} \quad (16)$$

#### 2. Specialized Detector Approach

Within the nonself detectors, subsets can be identified to correspond to specific categories of abnormal conditions for identification and evaluation. The approach implies the use of the NSS and a priori knowledge of specialized detectors. Such information can be obtained from tests, simulation, or analysis. In Fig. 13, this concept is illustrated for the two-dimensional case. PSS can also be applied to determine the sets of specialized detectors for known failures for which data is available.

#### 3. Hierarchical Multiself Strategy

This method applies to the identification and direct evaluation processes. It is based on the idea that not the entire  $n$ -dimensional space needed to capture the characteristics of all failures considered may be necessary for the different phases of the FDIE process, but lower size sets of identifiers may be used instead. The method is equivalent to investigating lower dimensional projections of the identifiers space. It is expected to increase efficiency and mitigate high-dimensionality issues. It requires identification of low dimension spaces for hierarchical selves definitions. Both PSS and NSS can be applied. In Fig. 14, the block diagram of the FDIE process using a hierarchical multiself strategy (HMS) is presented.

#### 4. Detection Logic

A binary output, match or not-match, is produced for each sample of the explored current data. In a very simple detection scheme this

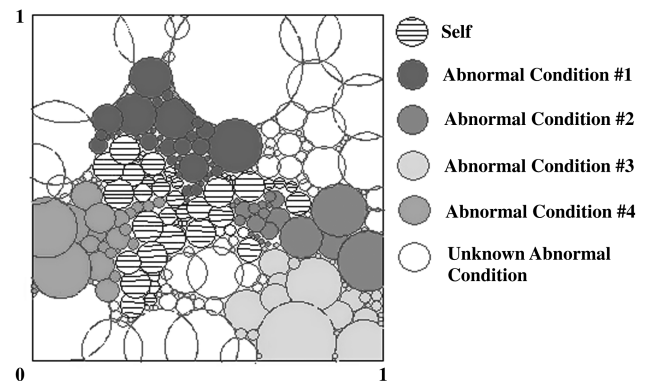


Fig. 13 Identification using the specialized detector approach.



could be used as FDI outcome but is likely to expose the process to high false alarm rates. Filtering out of inadequate false alarms can be achieved by producing the FDI outcome as a sequence of binary decisions based primarily on the number of detectors activated over a moving time window. It should be noted that some of the abnormal conditions are characterized by continuity and gradualness and that there are uncertainties introduced by data inconsistencies and insufficient coverage of self/nonself. In this context, it is expected that improved performance of the FDI scheme can be achieved through fuzzy logic-based decision algorithms. Areas where fuzzy logic is expected to provide adequate tools for FDIE include: 1) fuzzy detector boundaries implemented in the vicinity of the self; 2) fuzzy counting of triggered detectors; 3) fuzzy threshold for binary outcome involving additional metrics such as proximity to the self; and 4) overall fuzzy FDIE output based on internal propagation of fuzzy elements and previously obtained statistics of correct detections and false alarms.

### G. Evaluation of Failure

The qualitative evaluation of the failure can be performed by considering the type of the failure as an additional classification target and treating it similarly to an additional identification phase.

The direct evaluation or failure magnitude assessment can be approached at two levels of accuracy. An approximate magnitude assessment, using larger categories such as *small*, *medium*, and *large*, can be performed by considering an additional classification target within each identified abnormal condition. It is expected that a higher accuracy quantitative magnitude assessment with numerical outcomes is possible based on a combination of AIS algorithms and analytical estimates, provided that extensive experimental data are available.

The indirect evaluation or reduced flight envelope prediction must rely on a combined strategy based on analytical flight envelope reduction assessment and AIS-based approaches for parameter space reduction assessment. In this paper, a general meaning is attributed to the flight envelope, which includes all dynamic parameters and states that are of interest for performing specific piloting tasks and accomplishing specific missions. The analytical methods require accurate modeling of the failures and significant online computational capabilities. The AIS methods imply that all pertinent parameters to the flight envelope, considering its generalized meaning, are

part of the identifier sets. Let us assume that the self is defined as the set of all  $n$ -dimensional hyperspheres  $S_i$  characterized by the center  $c_i$  and the radius  $r_i$ :

$$S = \{(c_i, r_i)\} = \{S_i\}, \quad i = 1, 2, \dots, N_S \quad (17)$$

$$c_i = [x_1, x_2, \dots, x_n]^T_i \quad (18)$$

where  $N_S$  is the total number of clusters and  $n$  is the total number of identifiers that define the self. The self can be viewed as a generalized flight envelope. Assume that each failure  $F_k$  is defined by a set of constraints  $C$  on known variables  $x_{Fk}$ , with  $k = 1, 2, \dots, N_F$ :

$$C = C(x_{Fk}) \quad (19)$$

The variables  $x_{Fk}$  must be part of the identifier set:

$$\{x_{Fk}\}_{k=1,2,\dots,N_F} \subset \{x_j\}_{j=1,2,\dots,n} \quad (20)$$

Then a “new” self can be defined as

$$S_{\text{new}} = \{(c_i, r_i) | (c_i, r_i) \text{ satisfy } F\} \quad (21)$$

The concept is illustrated in Fig. 15 for the two-dimensional case.

### H. Reevaluation of Self

Completely and accurately defining the self is a challenging task. It is expected that some areas of the self will not be covered due to lack of test data and that some nonself regions will be included in the self during the detector generation process. For improved effectiveness, it is important to develop tools that are capable of tuning the sets of self or nonself detectors based on FDIE results and evaluation of results obtained during online operation. This should be regarded as a continuous optimization process. Primarily, tuning of the detector set can be performed through alteration of selected detector size, adding/removing detectors, and/or splitting detectors into several smaller ones. It should also be noted that obtaining adequate data to define the self over the entire envelope may occur in phases and the development of AIS detection schemes may be performed first over limited regions and later expanded when more data are available.

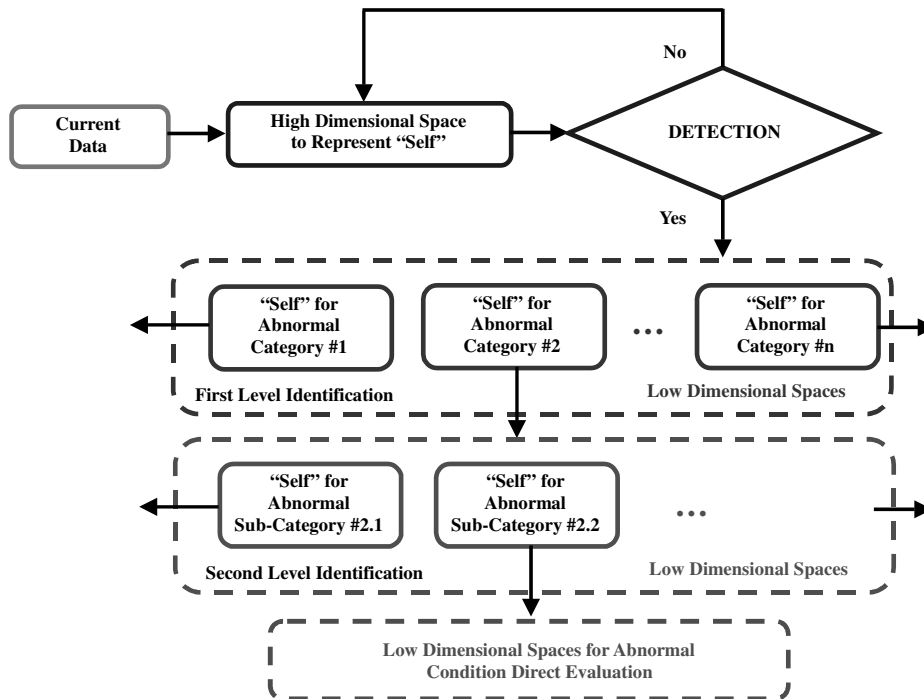


Fig. 14 Identification using the hierarchical multiself strategy.

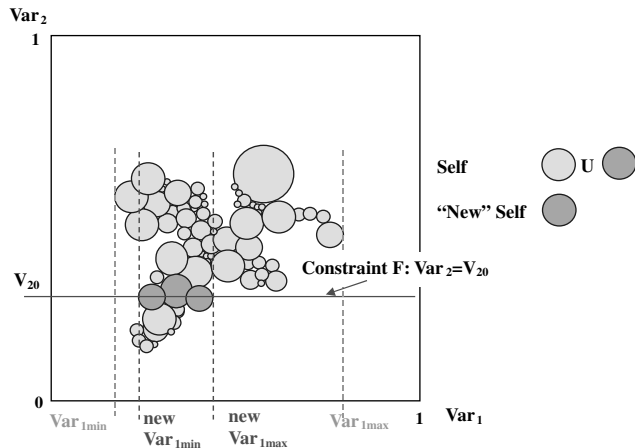


Fig. 15 Failure impact on envelope reduction using AIS.

## VI. Example of an AIS-Based FDI Scheme

Using data from the WVU motion-based flight simulator, an integrated AIS-based FDI scheme was developed using a HMS [48]. The proposed scheme was then tested and the capability of detecting and identifying several categories of subsystem abnormal conditions analyzed. Table 1 outlines the characteristics of the simulated failures considered. It should be noted that this example has the purpose to illustrate the implementation of the proposed framework and emphasize the potential benefits of using the HMS as an alternative to individual self configurations. Further improvements in detection performance can be achieved through optimization of the detector sets and/or modifications of the self configurations.

A subset of the flight envelope with three specific reference points was selected and different flight scenarios considered. At point 1, the aircraft is in steady state level flight (Mach 0.75 and 20,000 ft), ascends at constant speed to point 2 (Mach 0.75 and 31,000 ft), accelerates at constant altitude to point 3 (Mach 0.9 and 31,000 ft), and then returns to points 2 and 1. Several flight tests, lasting approximately 15 minutes each and covering the previously described envelope region, were designed to include steady state flight conditions, transitions between steady state conditions, and mild to moderate maneuvers such as doublets and coordinated turns with different bank angles. These flight scenarios were simulated under normal flight conditions. Then, they were repeated under various failure scenarios. Only one failure at a time is considered to capture/isolate the dynamic fingerprint of each type of failure. A distinct set of tests were used for scheme development purposes and a different

one for testing and validation. The data from the WVU motion-based flight simulator was acquired at a rate of 50 Hz.

The self or normal condition was defined as a set of hyperspherical clusters. Five different sets of identifiers were considered as listed in the Table 2. Corresponding detectors were generated for each self using real-valued representation and a negative selection algorithm with variable detector size without optimization. The performance of each individual self was first evaluated in terms of detection rate and false alarms. The detection rate was computed as the percentage of all data samples that triggered a detector for the entire data set in the presence of the respective failures. The false alarm rate was computed as the percentage of all data samples that triggered a detector for the entire data set at nominal conditions. Note that this was a different set of data than the one used to build the self. All these performance results for individual selves are presented in Table 3. It is important to notice that each self achieves very good performance for at least one class of failure and may have worse performance for the others. The fact that different selves favor the detection of particular types of failures is used, within the multiself strategy [48], to develop an integrated scheme where different self configurations ensure overall high detection rate and low number of false alarms.

The five selves were integrated in a logical scheme that attributed different decision privileges to each self depending on its particular detection capabilities. Once a failure condition is declared by the detection phase scheme, the identification phase starts to perform a preclassification according to the four failure categories considered. Within the nonself detectors, a subset of specialized detectors has been predetermined to correspond to specific categories of abnormal conditions. The detection outcome is a binary output (1 = failure, 0 = nominal) produced at the sampling rate based on a moving time window of width  $\omega = 5$  samples and a detection threshold of 40%, which represents the number of consecutive points over the window that trigger detectors, summed over all selves. The results for the failure detection are presented in Table 4. The false alarm metric represents now the percentage of all scheme outcomes of 1 at nominal conditions. The detection rate metric represents now the percentage of all scheme outcomes of 1 at failure conditions. As compared with the results presented in Table 3 for individual/isolated detector sets, the HMS improves the detection rate while decreasing the number of false alarms. For example, the average number of false alarms is reduced from 6.12% for the individual selves to 2.5% by using the HMS while the average number of detections is increased from 71.57 to 88.50%. These results confirm the fact that by using an integrated multiself scheme instead of considering self configurations separately, better detection performance can be achieved. Note that the engine failure is the only one that presents a lower detection rate. In fact, none of the eight selves outlined in the Table 2 achieves a very good detection performance for this type of failure. This is due

Table 1 Simulated failures

Failure category	Failure type	Description
Actuator	Stabilator, aileron, or rudder	Blockage of any, left, or right control surface at 8 deg
Sensor	Large fast drifting bias LFSB	Step bias of 10 deg/s in the roll and pitch rate gyro sensors and 3 deg/s in the yaw rate gyro sensor
Structural	Wing damage	Loss of 15% of any, left, or right wing, also affecting the "efficiency" of the aileron control surface
Engine	Power/thrust reduced control efficiency	Loss of the 98% of the power in any left of right engine.

Table 2 Identifier configurations for self definition

Self number	Identifiers	Solution space dimension
Self 1	$NN_{wp}, NN_{out}, MQEE, OQEE, \text{ and } DQEE_x$	9
Self 2	$NN_{wp}, NN_{out}$	4
Self 3	$NN_{out}$	3
Self 4	$DQEE_x$	3
Self 5	$NN_{out}, MQEE, OQEE, \text{ and } DQEE_x$	8

**Table 3 Detection performance of different self configurations**

Self configuration	Number of detectors	Failure test data detection rates, %							Nominal test data false alarms validation data, %
		Actuator failure 8 deg			Sensor failure		Structural failure	Engine failure	
		Stabilator	Aileron	Rudder	LSB	LFDB			
Self 1	499	L: 99.79 R: 99.98	L: 86.52 R: 70.62	L: 90.85 R: 71.81	p: 92.87 q: 92.01 r: 99.75	p: 87.62 q: 95.93 r: 99.38	L: 99.68 R: 99.84	L: 73.82 R: 36.32	2.49
Self 2	213	L: 99.97 R: 99.97	L: 96.84 R: 99.97	L: 97.01 R: 95.70	p: 69.59 q: 83.13 r: 98.03	p: 52.89 q: 87.06 r: 98.03	L: 99.98 R: 72	L: 72.30 R: 52.90	5.25
Self 3	516	L: 99.07 R: 99.97	L: 99.96 R: 99.96	L: 98.51 R: 96.39	p: 60.80 q: 94.93 r: 98.97	p: 41.02 q: 94.78 r: 99.28	L: 99.96 R: 87.34	L: 80.62 R: 34.19	19.59
Self 4	507	L: 6.44 R: 1.66	L: 0.23 R: 0.80	L: 0.91 R: 1.60	p: 92.74 q: 57.62 r: 99.73	p: 89.15 q: 27.78 r: 99.81	L: 12.44 R: 8.25	L: 0.84 R: 1.02	0.78
Self 5	504	L: 99.9 R: 99.9	L: 79.8 R: 57.8	L: 92.3 R: 76.9	p: 95.6 q: 90.5 r: 99.8	p: 90.8 q: 95.58 r: 99.8	L: 99.5 R: 99.9	L: 59.8 R: 10.8	2.5

**Table 4 Failure detection performance of the HMS strategy**

Window $\omega$ , samples	Detection threshold thr	<i>Failure test data detection rates, %</i>								Nominal test data false alarms validation data, %
		<i>Actuator failure</i>			<i>Sensor failure</i>		Structural Failure	Engine Failure		
		Stabilator	Aileron	Rudder	LSB	LFDB				
5	10	L: 100 R: 99.40	L: 99.27 R: 100	L: 97.75 R: 95.51	$p$ : 97.3 $q$ : 95.4 $r$ : 99.8	$p$ : 92.0 $q$ : 95.4 $r$ : 99.8	L: 100 R: 100	L: 77.3 R: 40.0	2.5	

**Table 5 Identification performance of the HMS strategy**

Failure type	Failure category (identification rates), %				
	Actuator	Sensor	Structural	Engine	Unknown
R: Stabilator	92	0	7	0	0
L: Aileron	99.81	0	0	0.13	0
R: Rudder	97.27	0.75	0.46	0.54	0.98
r: LSB	0	99.85	0	0	0
r: LFDB	0	100	0	0	0
p: LFDB	3	85	8	0.5	3.15
L: Structural	0.67	2.5	96.74	0	0

to the fact that additional identifiers possibly relevant to engine operation such as longitudinal acceleration and information on pilot throttle commands have not been considered as identifiers in this example.

Table 5 summarizes the results for the identification phase when the category of the failed element is specifically determined. Note that unknown abnormal conditions have been considered as well. This unknown condition is declared when some detectors are activated which have not been predetermined to belong to any of the specialized detector sets. A preliminary robustness analysis performed on a similar scheme [63] has revealed that the presence of high magnitude perturbations may be categorized as unknown abnormal conditions. For example, the scheme is robust to light turbulence ( $\sigma = 1.5$  m/s), but it will declare an unknown abnormal condition in the presence of severe turbulence ( $\sigma = 4.5$  m/s).

## VII. Conclusions

An integrated framework for the detection, identification, and evaluation of a wide variety of aircraft subsystems failures has been

developed based on the AIS paradigm. The proposed methodology is expected to mitigate the limitations of current approaches for aircraft subsystem FDIE regarding generality and robustness.

The general outline of a comprehensive FDIE process has been presented and the main components described and analyzed.

Critical issues related to the design of AIS-based FDIE schemes have been identified and potential solutions proposed.

An AIS-based multiself scheme is presented capable of detecting and identifying failures affecting aircraft actuators, sensors, structural integrity, and propulsion. Data from a motion-based flight simulator was used for development and validation. The scheme achieves excellent detection rates and number of false alarms for all normal and abnormal flight conditions considered over a significant segment of the flight envelope.

The AIS paradigm addresses directly the complexity and multi-dimensionality of aircraft dynamic response in the context of integrated abnormal condition detection, identification, and evaluation and provides adequate tools for a comprehensive solution to this problem.

## Acknowledgment

This research effort was sponsored by NASA Aviation Safety Program through a grant within the Integrated Resilient Aircraft Control project.

## References

- [1] "Annual Reviews of Aircraft Accident Data," National Transportation Safety Board Repts., 1983–2007, <http://www.nts.gov/Aviation/Stats.htm> [retrieved 28 Sept. 2010].
- [2] "General Aviation Accident Trends and Factors for 1997–2006," Aircraft Owners and Pilots Association, Nall Repts., 1997–2006, <http://www.aopa.org/asf/publications/nall.html> [retrieved 28 Sept. 2010].
- [3] Aviation Safety Database 1943–2008, Flight Safety Foundation, <http://aviation-safety.net/database/> [retrieved 28 Sept. 2010].

- [4] "Accident/Incident Data System," Federal Aviation Administration, 1978–2007, [http://www.asias.faa.gov/portal/page/portal/ASIAS\\_PAGES/ASIAS\\_HOME/DATAINFO/DATABASES:A-E](http://www.asias.faa.gov/portal/page/portal/ASIAS_PAGES/ASIAS_HOME/DATAINFO/DATABASES:A-E) [retrieved 28 Sept. 2010].
- [5] White, J., "NASA's Aviation Safety Program," 44th Annual AIAA Aerospace Sciences Meeting, Reno, NV, 9–12 Jan. 2006.
- [6] KrishnaKumar, K., and Gundy-Burlet, K., "Intelligent Control Approaches for Aircraft Applications," JANAFF Interagency Propulsion Committee Meeting, Destin, FL, 2002.
- [7] KrishnaKumar, K., "Intelligent Systems for Aerospace Engineering: An Overview," von Karman Lecture Series on Intelligent Systems for Aeronautics, Rhode-Saint-Genèse, Belgium, May 2002.
- [8] Wilsky, A. S., "Failure Detection in Dynamic Systems," AGARD LS-109, Neuilly sur Seine, France, Oct. 1980, 2.1–2.14.
- [9] Marcos, A., Ganguli, S., and Balas, G., "Application of Fault Detection and Isolation to a Boeing 747-100/200 Aircraft," AIAA Guidance, Navigation and Control Conference, AIAA Paper 02-4944, Aug. 2002.
- [10] Shin, J. Y., Wu, N. E., and Belcastro, C., "Linear Parameter Varying Control Synthesis for Actuator Failure, Based on Estimated Parameter," AIAA Guidance, Navigation and Control Conference, AIAA Paper 02-4546, Aug. 2002.
- [11] Narendra, K. S., and Balakrishnan, J., "Adaptive Control Using Multiple Models," *IEEE Transactions on Automatic Control*, Vol. 42, No. 2, 1997, pp. 171–187. doi:10.1109/9.554398
- [12] Napolitano, M. R., Casdorph, V., Neppach, C., and Naylor, S., "On-Line Learning Neural Architectures and Cross-Correlation Analysis for Actuator Failure Detection and Identification," *International Journal of Control*, Vol. 63, No. 3, 1996, pp. 433–455. doi:10.1080/00207179608921851
- [13] Jakubek, S., and Strasser, T., "Fault Diagnosis Using Neural Networks with Ellipsoidal Basis Functions," *Proceedings of the American Control Conference*, Anchorage, AK, 2002, pp. 3846–3851.
- [14] Lou, S. J., Budman, H., and Duever, T. A., "Comparison of Fault Detection Techniques: Problem and Solution," *Proceedings of the American Control Conference*, Anchorage, AK, 2002, pp. 4513–4518.
- [15] Napolitano, M. R., Young, A., and Seanor, B., "A Fault Tolerant Flight Control System for Sensor and Actuator Failures Using Neural Networks," *Aircraft Design*, Vol. 3, No. 2, 2000, pp. 103–128.
- [16] Iverson, D., "Inductive System Health Monitoring," *Proceedings of the 2004 International Conference on Artificial Intelligence (IC-AI'04)*, Las Vegas, NV, 2004, pp. 605–611.
- [17] Napolitano, M. R., Neppach, C. D., Casdorph, V., Naylor, S., Innocenti, M., and Silvestri, G., "A Neural-Network-Based Scheme for Sensor Failure Detection, Identification, and Accommodation," *Journal of Guidance, Control, and Dynamics*, Vol. 18, No. 6, 1995, pp. 1280–1286. doi:10.2514/3.21542
- [18] Perhinschi, M. G., Napolitano, M. R., Campa, G., and Fravolini, M. L., "Integration of Fault Tolerant System for Sensor and Actuator Failures Within the WVU NASA F-15 Simulator," AIAA Guidance, Navigation, and Control Conference, Austin TX, Aug. 2003.
- [19] Nguyen, N., KrishnaKumar, K., Kaneshige, J., and Nespeca, P., "Dynamics and Adaptive Control for Stability Recovery of Damaged Asymmetric Aircraft," AIAA Guidance, Navigation, and Control Conference and Exhibit, Keystone, CO, Aug. 2006.
- [20] Tessler, A., "Structural Analysis Methods for Structural Health Management of Future Aerospace Vehicles," NASA TM-2007-214871, Langley Research Center, Hampton, VA, 2007.
- [21] Perhinschi, M. G., Napolitano, M. R., Campa, G., Fravolini, M. L., and Seanor, B., "Integration of Sensor and Actuator Failure Detection, Identification, and Accommodation Schemes Within Fault Tolerant Control Laws," *Control and Intelligent Systems*, Vol. 35, No. 4, Dec. 2007, pp. 309–318.
- [22] Totah, J., KrishnaKumar, K., and Viken, S., "Stability, Maneuverability, and Safe Landing in the Presence of Adverse Conditions," *Integrated Resilient Aircraft Control Technical Plan, Aviation Safety Program, Aeronautics Research Mission Directorate* [NASA website], [http://www.aeronautics.nasa.gov/nra\\_pdf/irac\\_tech\\_plan\\_c1.pdf](http://www.aeronautics.nasa.gov/nra_pdf/irac_tech_plan_c1.pdf) [retrieved 28 Sept. 2010].
- [23] Srivastava, A. N., Mah, R. W., and Meyer, C., "Automated Detection, Diagnosis, Prognosis to Enable Mitigation of Adverse Events During Flight," *Integrated Vehicle Health Management Technical Plan, Aviation Safety Program, Aeronautics Research Mission Directorate* [NASA website], [http://www.aeronautics.nasa.gov/nra\\_pdf/ivhm\\_tech\\_plan\\_c1.pdf](http://www.aeronautics.nasa.gov/nra_pdf/ivhm_tech_plan_c1.pdf) [retrieved 28 Sept. 2010].
- [24] Young, S. D., and Quon, L., "Integrated Intelligent Flight Deck," *Integrated Intelligent Flight Deck Technical Plan, Aviation Safety Program, Aeronautics Research Mission Directorate* [NASA website], [http://www.aeronautics.nasa.gov/nra\\_pdf/iifd\\_tech\\_plan\\_c1.pdf](http://www.aeronautics.nasa.gov/nra_pdf/iifd_tech_plan_c1.pdf) [retrieved 28 Sept. 2010].
- [25] Young, R., and Rohn, D., "Aircraft Aging and Durability Project," *Aircraft Aging and Durability Project Technical Plan, Aviation Safety Program, Aeronautics Research Mission Directorate* [NASA website], [http://www.aeronautics.nasa.gov/nra\\_pdf/aad\\_tech\\_plan\\_c1.pdf](http://www.aeronautics.nasa.gov/nra_pdf/aad_tech_plan_c1.pdf) [retrieved 28 Sept. 2010].
- [26] KrishnaKumar, K., "Artificial Immune System Approaches for Aerospace Applications," 41st Aerospace Sciences Meeting and Exhibit, AIAA Paper 2003-0457, 2003.
- [27] Dasgupta, D., KrishnaKumar, K., Wong, D., and Berry, M., "Negative Selection Algorithm for Aircraft Fault Detection," *Proceedings from the 3rd International Conference on Artificial Immune Systems 2004*, edited by G. Nicosia et al., Catania, Sicily, Italy, 13–16 Sept. 2004, pp. 1–13.
- [28] Benjamini, E., *Immunology, A Short Course*, Wiley-Liss, New York, 1992.
- [29] Farmer, J., Norman, H., Packard, S., and Perelson, A. S., "The Immune System, Adaptation, and Machine Learning," *Physica D* [online journal], Vol. 22, Nos. 1–3, 1986, pp. 187–204 [retrieved 28 Sept. 2010]. doi:10.1016/0167-2789(86)90240-X
- [30] Forrest, S., Perelson, A. S., Allen, L., and Cherukuri, R., "Self-Nonself Discrimination in a Computer," *Proceedings of the IEEE Symposium on Research in Security and Privacy*, IEEE Computer Society Press, Los Alamitos, CA, 1994, pp. 202–212.
- [31] Dasgupta, D., and Attouh-Okine, N., "Immunity-Based Systems: A Survey," *IEEE International Conference on Systems, Man, and Cybernetics*, Vol. 1, Orlando, FL, 12–15 Oct. 1997, pp. 396–374.
- [32] Dasgupta, D., and Forrest, S., "Artificial Immune Systems in Industrial Applications," *Proceedings of the Second International Conference on Intelligent Processing and Manufacturing of Materials*, Vol. 1, Honolulu, HI, 10–15 July 1999, pp. 257–267.
- [33] Zhi-Tang, L., Yao, L., and Li, W., "A Novel Fuzzy Anomaly Detection Algorithm Based on Artificial Immune System," *Proceedings of the Eighth International Conference on High-Performance Computing in Asia-Pacific Region (HPCASIA'05)*, 2005, 1 July 2005, pp. 481–486.
- [34] D'haeseleer, P., Forrest, S., and Helman, P., "An Immunological Approach to Change Detection: Algorithms, Analysis and Implications," *IEEE Symposium on Security and Privacy*, Oakland, CA, 6–8 May 1996, pp. 110–119.
- [35] Dasgupta, D., and Nino, F., "Comparison of Negative and Positive Selection Algorithms in Novel Pattern Detection," *Proceedings of the IEEE International Conference on Systems, Man and Cybernetics*, Vol. 1, Nashville, TN, 8–11 Oct. 2000, pp. 125–130.
- [36] De Castro, L., and Timmis, J., "Artificial Immune Systems: A Novel Paradigm to Pattern Recognition," *Artificial Neural Networks in Pattern Recognition*, edited by J. M. Corchado, L. Alonso, and C. Fyfe, Univ. of Paisley, Paisley, England, U.K., 2002, pp. 67–84.
- [37] Dasgupta, D., and Forrest, S., "Novelty Detection in Time Series Data Using Ideas from Immunology," *International Conference on Intelligent Systems*, Reno, NV, 1996.
- [38] Dasgupta, D., and Majumdar, N., "Anomaly Detection in Multidimensional Data Using Negative Selection Algorithm," *Proceedings of the Congress on Evolutionary Computation CEC '02*, Vol. 02, 2002, pp. 1039–1044.
- [39] Kim, J., Greensmith, J., Twycross, J., and Aickelin, U., "Malicious Code Execution Detection and Response Immune System Inspired by the Danger Theory," *Adaptive and Resilient Computing Security Workshop (ARCS-05)*, Santa Fe, NM, 2005.
- [40] De Castro, L., and Timmis, J., "Artificial Immune Systems as a Novel Soft Computing Paradigm," *Soft Computing Journal*, Vol. 8, No. 7, 2003, pp. 526–544.
- [41] Gonzalez, F., Dasgupta, D., and Kizma, R., "An Immunogenetic Technique to Detect Anomalies in Network Traffic," *Proceedings from the Genetics and Evolutionary Computation Conference*, New York, 9–13 July 2002, pp. 1081–1088.
- [42] Ko, A., Lau, H., and Lau, T., "An Immune Control Framework for Decentralized Mechatronic Control," *Proceedings of the Third International Conference on Artificial Immune Systems*, Catania, Sicily, Italy, 13–16 Sept. 2004, pp. 91–105.
- [43] Karr, C., Nishita, K., and Graham, K., "Adaptive Aircraft Flight Control Simulation Based on an Artificial Immune System," *Applied Intelligence: The International Journal of Artificial Intelligence, Neural Networks, and Complex Problem-Solving Technologies*, Vol. 23, No. 3, Dec. 2005, pp. 295–308. doi:10.1007/s10489-005-4614-z
- [44] Stibor, T., Timmis, J., and Eckert, C., "On the Appropriateness of Negative Selection Defined over Hamming Shape-Space as a Network

- Intrusion Detection System," *Proceedings of the Fourth International Conference on Artificial Immune Systems*, 2006.
- [45] Ji, Z., and Dasgupta, D., "Applicability Issues of the Real-Valued Negative Selection Algorithms," *Proceedings for the Genetics and Evolutionary Computation Conference, 2006*, Seattle, WA, 8–12 July 2006, pp. 111–118.
- [46] Perhinschi, M. G., Napolitano, M. R., Campa, G., Seanor, B., Burken, J., and Larson, R., "An Adaptive Threshold Approach for the Design of an Actuator Failure Detection and Identification Scheme," *IEEE Transactions on Control Systems Technology*, Vol. 14, No. 3, May 2006, pp. 519–525.  
doi:10.1109/TCST.2005.860522
- [47] Perhinschi, M. G., and Moncayo, H., "Integrated System for Immunity-Based Failure Detection, Identification, and Evaluation," NASA Integrated Resilient Adaptive Control Project, Project Progress Rept., Nov. 2008.
- [48] Moncayo, H., Perhinschi, M. G., and Davis, J., "Immunity-Based Aircraft Failure Detection and Identification Using an Integrated Hierarchical Multi-Self Strategy," AIAA Guidance, Navigation, and Control Conference, Chicago, IL, Aug. 2009.
- [49] Verleysen, M., and François, D., *The Curse of Dimensionality in Data Mining and Time Series Prediction*, Springer-Verlag, Berlin, 2005, pp. 758–770.
- [50] Charu, C. A., Hinneburg, A., and Keim, D., "On the Surprising Behavior of Distances Metrics in High Dimensional Space," IBM T. J. Watson Research Center, 2000.
- [51] Van Der Maaten, L. J. P., "An Introduction to Dimensionality Reduction Using MATLAB," Universiteit Maastricht, Maastricht, The Netherlands, July 2007.
- [52] Shapiro, J., Gary, B., and Peterson, G., "An Evolutionary Algorithm to Generate Hyperellipsoid Detectors for Negative Selection," *Proceedings of the Genetics and Evolutionary Computation Conference*, Washington, DC, 2005, pp. 337–344.
- [53] Balachandran, S., "Multi-Shaped Detector Generation Using Real Valued Representation for Anomaly Detection," Univ. of Memphis, Memphis, TN, Dec. 2005.
- [54] D'haeseleer, P., Forrest, S., and Helman, P., "An Immunological Approach to Change Detection: Algorithms, Analysis, and Implications," *Proceedings of the IEEE Symposium on Computer Security and Privacy*, Oakland, CA, 1996, pp. 110–119.
- [55] Gonzalez, F., and Dasgupta, D., "Anomaly Detection Using Real-Valued Negative Selection," *Genetic Programming and Evolvable Machines*, Vol. 4, No. 4, Dec. 2003, pp. 383–403.  
doi:10.1023/A:1026195112518
- [56] Gonzalez, F., Dasgupta, D., and Niño, L., "A Randomized Real-Valued Negative Selection Algorithm," *Proceedings of the 2nd International Conference on Artificial Immune Systems*, Edinburgh, U.K., 2003, pp. 261–272.
- [57] Gonzalez, F., Dasgupta, D., and Gomez, J., "The Effect of Binary Matching Rules in Negative Selection," *Proceedings of the Genetic and Evolutionary Computation Conference (GECCO 2003)*, edited by E. Cantu-Paz et al., Springer, Chicago, IL, 2003, pp. 195–206.
- [58] Zhang, J., and Zhao, M., "Hybrid Detector Set: Detectors with Different Affinity," Third International Conference on Information Security, Shanghai, China, 14–16 Nov. 2004.
- [59] Karr, C., Nishita, K., and Kenneth, S., "Adaptive Aircraft Flight Control Simulation Based on an Artificial Immune System," *Applied Intelligence: The International Journal of Artificial Intelligence, Neural Networks, and Complex Problem-Solving Technologies*, Vol. 23, No. 3, Dec. 2005, pp. 295–308.  
doi:10.1007/s10489-005-4614-z
- [60] Davis, J., Perhinschi, M. G., and Moncayo, H., "Evolutionary Algorithm for Artificial Immune System-Based Failure Detector Generation and Optimization," AIAA Guidance, Navigation, and Control Conference, Chicago, IL, Aug. 2009.
- [61] "Computational Science Education Project. Introduction to Monte Carlo Methods," Oak Ridge National Lab., 1995, <http://www.phy.ornl.gov/csep/CSEP/MC/MC.html> [retrieved 28 Sept. 2010].
- [62] Harmer, P., Williams, G., Gunsch, G., and Lamont, G., "An Artificial Immune System Architecture for Computer Security Applications," *IEEE Transactions on Evolutionary Computation*, Vol. 6, No. 3, June 2002, pp. 252–280.  
doi:10.1109/TEVC.2002.1011540
- [63] Moncayo, H., "Immunity-Based Detection, Identification, and Evaluation of Aircraft Subsystem Failures," Ph.D. Thesis, West Virginia Univ., Morgantown, WV, Dec. 2009.